Comment to Shreve & Delgado [2023] - "*Trapdoor Fault Activation: A Step Toward Caldera Collapse at Sierra Negra, Galapagos, Ecuador*"

Peter C. LaFemina[1,2], Andrew F. Bell[3], Patricia M. Gregg[4], William W. Chadwick Jr[5], Dennis Geist[6], Machel Higgins[7]

[1] Alfred Wegener Institute, Helmholtz Center for Polar & Marine Research, Bremerhaven, Germany
[2] Faculty of Geosciences, University of Bremen, Bremen, Germany
[3] School of Geosciences, University of Edinburgh, Edinburgh, Scotland
[4] Dept. of Earth Science & Environmental Change, University of Illinois Champaign Urbana, Urbana, Iillinois, 61801
[5] Oregon State University, CIMERS, Hatfield Marine Science Center, Newport, OR, 97365
[6] Geology Department, Colgate University, Hamilton NY 13346
[7] Institute of Environment, Florida International University, Miami, FL 33199

Corresponding author: Peter LaFemina (mailto:peter.lafemina@awi.de)

Key Points:

- The 2005-2018 eruptive cycle at Sierra Negra volcano resulted in ~2.0 m net resurgence of the Sinuous Ridge – Trapdoor Fault system.
- Shreve & Delgado [2023] hypothesize the initiation of caldera collapse during the 2018 eruption because they focus on co-eruptive deformation, and not the entire eruptive cycle.
- Resurgence of basaltic calderas is rare making the 2005 and 2018 Sierra Negra resurgent events important to study.

Abstract

In their article entitled “*Trapdoor Fault Activation: A Step Toward Caldera Collapse at Sierra Negra, Galapagos, Ecuador*” *Shreve and Delgado* [2023] examine co-eruptive deformation during the 2018 eruption of Sierra Negra Volcano. One of their major conclusions is that the 2018 eruption, and specifically co-eruptive faulting, represents the initial stages of caldera collapse. They reach this conclusion because they focus their analysis solely on co-eruptive deformation, and do not investigate the total (net) deformation for the 2005 to 2018 eruption cycle. *Bell et al.* [2021c] investigated both the pre- and co-eruptive phases of the 2018 eruption and showed that net deformation was one of caldera resurgence, not subsidence. In this comment, we demonstrate that the conclusion of collapse, or even initiation of collapse, is attributable to not accounting for pre-eruptive deformation on the intra-caldera Trapdoor Fault system and incorrectly assuming that the volcano-tectonic dynamics of Sierra Negra mimic those of other basaltic calderas.

Plain Language Summary

Volcanoes deform before, during and after eruptive episodes. If one studies just one of these periods, a complete understanding of the deformation history is missed and incorrect conclusions can be drawn about an eruptive episode. In their article entitled “*Trapdoor Fault Activation: A Step Toward Caldera Collapse at Sierra Negra, Galapagos, Ecuador*” *Shreve and Delgado* [2023] examine only the co-eruptive deformation during the 2018 eruption of Sierra Negra Volcano. Based on their analysis they conclude that the 2018 eruption, and specifically co-eruptive faulting, represents the initial stages of caldera collapse. However, this conclusion is only reached by not accounting for extensive pre-eruptive deformation that occurred in the lead up to the eruption on 26 June 2018. In this comment, we demonstrate that the conclusion of collapse or even initiation of collapse is attributable to not including the entire eruptive episode and net deformation on the intra-caldera Trapdoor Fault system in their analysis.

1 Introduction

Calderas form by mechanical collapse of a volcanic edifice on steeply dipping, caldera bounding ring faults that penetrate toward the magmatic system (e.g., [*Branney*, 1995]). Collapse is induced by the evacuation of magma from a crustal magma reservoir through eruption or intrusion. After collapse, caldera systems may experience structural resurgence characterized by the uplift of the caldera floor, hypothesized to be induced by intrusion of new magma into the remnants of pre-caldera magmatic reservoirs [*Marsh*, 1984]. Structural resurgence is typically associated with felsic systems where it occurs over protracted time scales, thousands of years or longer, and results in permanent doming of the caldera floor and/or uplift of faulted blocks >100 m above the caldera floor (e.g., [*de Silva et al.*, 2015; *Galetto et al.*, 2017]). On the other hand, resurgence is relatively rare at basaltic calderas [*Acocella et al.*, 2024; *Branney and Acocella*, 2015; *Galetto et al.*, 2017]. The three known cases of resurgence observed at basaltic calderas include: 1) Siwi caldera, Vanuatu [*Brothelande et al.*, 2016; *Métrich et al.*, 2011]; and 2) Alcedo [*Galetto et al.*, 2019] and 3) Sierra Negra calderas [*Bell et al.*, 2021c; *Galetto et al.*, 2019], Galapagos Islands, Ecuador. Siwi caldera is basaltic to trachy-andesitic in composition, and resurgence is mechanically similar to that observed at more felsic systems. Alcedo and Sierra Negra are basaltic ocean island volcanoes and resurgence takes place on intra-caldera faults systems [*Bell et al.*, 2021c; *Galetto et al.*, 2019].

The 2005 to 2018 eruption cycle of Sierra Negra provides one of the first opportunities to study the volcano-tectonic response of a basaltic caldera to pre- and co-eruptive deformation, including resurgence [*Bell et al.*, 2021c; *Chadwick et al.*, 2006]. The eruption cycle was monitored geodetically by a 10-station cGPS network, two tiltmeters, and multiple SAR satellites, seismically by a 6-station permanent seismic network, a temporary deployment of 9 seismometers, and global seismic networks, and using geologic and geochemical observations. New observations of dynamic caldera processes included: 1) the largest historically recorded pre-eruptive inflation (>6.5 m) and co-eruptive deflation (~8.5 m) without surface rupture or displacements on the ring fault system (i.e., elastic deformation of the caldera floor/reservoir roof); 2) correlation of uplift (inflation) and subsidence (deflation) rates with intra-caldera seismicity rates; 3) a reversal in slip polarity on the intra-caldera Trapdoor Fault system (TDF) from uplift during pre-eruptive events to subsidence during co-eruptive events; and 4) net uplift (resurgence) of ~2.0 m of the Sinuous Ridge along the TDF (Table 1; Bell et al., 2021a). The intra-caldera Sinuous Ridge has formed over time by displacements on the TDF and has been vertically displaced higher than the caldera rim, indicating that resurgence has been a dominant volcano-tectonic process for over the past ~1000 years [Figure 1; [*Bell et al.*, 2021c; *Reynolds et al.*, 1995]]. These observations are contrary to the analysis presented by *Shreve and Delgado* [2023] in which caldera collapse or the initiation of collapse during the 2018 eruption was hypothesized. Simply stated, the 2005 to 2018 magmatic cycle at Sierra Negra Volcano, Galapagos Islands resulted in net uplift (resurgence) of the caldera, not caldera collapse.

Shreve and Delgado [2023] utilized remotely sensed data, including optical satellite imagery, InSAR and cGPS, to estimate the volume of erupted products and to quantify deformation during the *co-eruptive* phase of the 2018 eruption. Their findings are complementary to existing observations (e.g., [*Bell et al.*, 2021c; *Vasconez et al.*, 2018]) and provide new quantitative estimates of erupted volume and co-eruptive processes, mainly the magnitude and location of the co-eruptive deflation source and displacements on the TDF due to the earthquakes on 5 July 2018 M_w5.1 and 22 July 2018 m_b 4.6 (Global Centroid Moment Tensor Catalog (GCMT): [*Dziewonski et al.*, 1981; *Ekström et al.*, 2012]; National Earthquake Information Center (NEIC): *www.earthquakes.usgs.gov*) (Table 1). *Shreve and Delgado* [2023] presented daily and 5-minute cGPS time series solutions from stations within the caldera (see *Shreve and Delgado* [2023] Figure 3a & Supplementary Materials; GPS analyses were also provided by P. LaFemina and M. Higgins). The deformation observed in these time series and specifically the co-seismic displacements for the 26 June 2018 M_w5.3 pre-eruptive earthquake were not accounted for during the analysis of displacements on the TDF, however. By focusing solely on the co-eruptive period, the analysis presented in *Shreve and Delgado* [2023] misses critical aspects of the volcano-tectonic response of the Sierra Negra caldera during the 2005-2018 eruption cycle, mainly that of net uplift of the Sinuous Ridge and therefore resurgence.

Shreve and Delgado [2023] concluded that Sierra Negra's caldera experienced ~-1.5 m of net subsidence on the intra-caldera TDF due to the 2018 eruption and co-eruptive earthquakes.

Their approach to determining the magnitude of deformation first assumed that -2.0 m of slip occurred on the TDF system, based on the difference between the observed 6.5 m of pre-eruptive inflation and -8.5 m of co-eruptive deflation. They modeled the -8.5 m of co-eruptive deflation as observed in InSAR interferograms assuming an elastic response to a deflating sill located at ~2.0 km depth (e.g., [*Bell et al.*, 2021c; *Chadwick et al.*, 2006; *Geist et al.*, 2008; *Jonsson et al.*, 2005; *Yun et al.*, 2006]). The residual displacements between the best-fit magmatic deformation model and the InSAR observations suggest: 1) the -8.5 m of subsidence was accommodated elastically; and 2) additional deformation on the TDF, consistent with co-eruptive seismicity (e.g., [*Bell et al.*, 2021a; *Bell et al.*, 2021c]). The model residuals located along the TDF, termed 'faulting residuals' in *Shreve and Delgado* [2023], were then modeled to estimate co-seismic slip accompanying the co-eruptive earthquakes. As an aside, the model residuals and therefore the estimates of co-seismic slip strongly depend on the parameters of the magmatic source model, but no parameter uncertainties for either the magmatic source or the faulting models were provided. Inversion of the model residuals for slip on a vertical TDF resulted in downward displacements of -1.1 m for the 5 July 2018 event and -0.35 m for the 22 July 2018 event [*Shreve and Delgado*, 2023]. These results are consistent with observed normal-faulting focal mechanisms presented in [*Bell et al.*, 2021a; *Bell et al.*, 2021c], but are greater than the maximum observed displacements at cGPS station GV06 of -0.57 m and -0.10 m, for the two events (Table 1). Based mainly on these modeling results, which assume -2 m of caldera floor subsidence at the outset, and additional estimates of minor co-seismic displacements on the northern and western segments of the TDF, *Shreve and Delgado* [2023] suggest that the 2018 eruptive episode resulted in ~-1.5 m of net motion on the TDF. The authors then interpret their derived net subsidence as the initiation of caldera collapse at Sierra Negra. Furthermore, the authors assume that the residual ~-0.5 m of displacement (i.e., difference between the -2.0 m of assumed slip and the ~-1.5 m modeled slip) occurred via aseismic slip on the TDF. This conclusion is reached despite its inconsistency with the cGPS time series.

It is our position that interpretation of deformation data during any eruptive episode, and specifically the 2018 eruption of Sierra Negra, is likely to lead to incorrect conclusions regarding the volcano-tectonic system, unless the entire eruptive cycle is considered. The previous two eruptions of Sierra Negra occurred in 2005 and 1979. Space geodesy measurements became available in the early 1990s, and a continuous GPS network was established in 2000 [*Chadwick et al.*, 2006; *Geist et al.*, 2006]. This network allowed for investigation of a complete eruptive cycle from the end of the 2005 eruption to the end of the 2018 eruption (Figure 3), including pre-eruptive deformation on the TDF (Figure 4). In the following, we first describe geophysical and geologic observations for the 2005 eruption that indicate resurgence of the caldera along the Sinuous Ridge – TDF system. We then describe the geophysical and geologic evidence as presented in *Bell et al.* [2021c] and *Bell et al.* [2021a] that indicates the Sierra Negra caldera experienced net resurgence of ~2.0 m along the Sinuous Ridge - TDF system during the 2018 eruptive event, not the ~-1.5 m subsidence as suggested by *Shreve and Delgado* [2023]. Therefore, even partial initiation of caldera collapse did not take place in 2018. Rather the caldera at Sierra Negra remains in an era of protracted resurgence.

2 The 2005 to 2018 Eruption Cycles: Geodetic, Seismic & Geologic Evidence for Caldera Resurgence

The 2005 eruption of Sierra Negra was preceded by >5 m of uplift at the center of the caldera [*Chadwick et al.*, 2006; *Geist et al.*, 2008]. This is a minimum estimate, as geodetic monitoring only began in 1992 (i.e., there are no observations from 1979-1992). Regional and global seismic networks, as well as analyses of InSAR data, observed multiple M>4 earthquakes leading up to the eruption, including the 11 January 1998 M_w 5.0 (NEIC) with an estimated 1.2 m of vertical displacement on the TDF [*Amelung et al.*, 2000], the 16 April 2005 M_b4.6 earthquake with ~0.84 m vertical displacement on the southern TDF [*Jonsson*, 2009] and a M_w5.5 earthquake approximately three hours before the onset of the 22 October 2005 eruption that displaced the southern TDF ~1.5 m (Figure 2; [*Chadwick et al.*, 2006; *Geist et al.*, 2008]). The central caldera floor subsided co-eruptively ~5 m as measured at cGPS station GV02 and began to uplift immediately following the cessation of eruptive activity (Figures 1 & 3; [*Chadwick et al.*, 2006; *Geist et al.*, 2008]). Uplift over the next 13-years was not steady and occurred in four main phases, with phases two and three separated by a brief period of deflation in 2012 (Figure 3). Short-term deflation events within long-term inflation episodes also occurred before the 2005 eruption [*Geist et al.*, 2008] and indicate either a lull in the magma supply and degassing, or deep lateral intrusion. The last phase of uplift before the 2018 eruption initiated in 2014, and in 2017 the rate increased dramatically to >1 m/yr, correlated in time with the onset of enhanced seismicity on the TDF [*Bell et al.*, 2021a; *Bell et al.*, 2021c].

A 9-station temporary seismic network was installed approximately 2 months before the 2018 eruption. This network and two local seismic stations allowed for enhanced detection and analysis of seismicity at Sierra Negra during the 2018 eruption [*Bell et al.*, 2021a; *Bell et al.*, 2021c]. Twenty-four M >4 earthquakes were recorded during the pre-eruptive (12) and co-eruptive (12) phases of 2018 activity. All of these earthquakes were located on the TDF and had focal mechanism solutions indicating reversal of slip directions between the two phases of activity, as well as complex slip directions depending on the hypocentral location of the earthquakes along the TDF [*Bell et al.*, 2021a; *Bell et al.*, 2021c; *Sandanbata et al.*, 2021]. Earthquakes with M >4 did not change the rate of inflation or deflation of the magmatic system [*Bell et al.*, 2021c]. However, earthquakes with M >4 on the TDF changed the state of stress on the TDF, as observed through a reduction in the number of earthquakes [*Bell et al.*, 2021a; *Bell et al.*, 2021b]. The three largest of the 24 M >4 2018 earthquakes account for the majority of seismic moment release and observed co-seismic displacements. These earthquakes are the: 1) pre-eruptive 26 June 2018 M_w 5.3, and 2) co-eruptive 5 July 2018 M_w5.1 and 3) 22 July 2018 m_b4.6 earthquakes [Table 1; Bell et al., 2021; Sandanbatta et al., 2021].

The rapid sequence of pre- and co-eruptive deformation, which included changes in the rate and polarity of deformation, were well-detected by the cGPS network. The temporal aliasing of InSAR observations; however, means that crucial details of the eruption cycle were missed and/or difficult to retrieve through modeling of the volcanic system using InSAR data alone. Specifically, pre-eruptive and co-eruptive deformation observed in the cGPS time series on 26 June 2018 included: 1) co-seismic displacements >1.0 m on the TDF (see below); 2) dike migration from the sill to eruptive fissures displaced cGPS station GV03 >1.0 m vertically and southward; and 3) rapid subsidence of the caldera floor correlated in time with intrusion initiation and eruption onset (Figure 4; [*Bell et al.*, 2021c]). *Shreve and Delgado* [2023] modeled the residuals (i.e., "faulting residuals") from their elastic, magmatic source deformation model of the InSAR data to estimate co-seismic displacements for the two largest co-eruptive earthquakes. In contrast, *Bell et al.* [2021c] quantified co-seismic displacements on the southern TDF using 30-sec kinematic position solutions for cGPS stations located on and across the TDF (i.e., stations GV06 and GV09, and GV08, respectively) (Figures 1 & 4; Table 1; [*Bell et al.*, 2021c]). That is, they investigated the co-seismic displacements directly with cGPS time series, and not through modeling of model residuals. An illustrative example is the pre-eruptive 9:15 UTC 26 June 2018 M_w 5.3 (GCMT) earthquake, which occurred on the southern segment of the TDF and had a reverse-faulting focal mechanism. *Bell et al.* [2021c] estimated 1.83 m and 1.43 m of vertical co-seismic displacements at stations GV09 and GV06 (these stations are located at the top of the inner-most fault scarp of the TDF system) (Figure 1). Station GV08, located on the outer-most block of the TDF fault system, was displaced downward -0.26 m. Therefore, the total throw across the TDF system during the 26 June 2018 M_w5.3 earthquake was 2.09 m and 1.69 m, for the GV09-GV08 and GV06-GV08 station pairs (Table 1).

Seismicity during the co-eruptive phase was dominated by normal-faulting focal mechanism solutions (i.e., downward displacement of the interior block), although some earthquakes exhibited thrust and strike-slip mechanisms [*Bell et al.*, 2021a]. The 5 July 2018 M_w5.1 co-eruptive earthquake was the second largest earthquake in the eruptive cycle. We estimated -0.14 m and -0.71 m co-seismic displacements from 30-sec kinematic solutions at cGPS stations GV09 and GV06, and 0.14 m at GV08, indicating a total throw of 0.0 m and -0.57 m (Table 1). The 22 July 2018 m_b 4.6 earthquake displaced stations GV09 and GV06 an estimated -0.08 m and -0.13 m, and GV08 0.03 m, indicating a total throw of -0.05 m and -0.10 m (Table 1). The change in location of maximum displacement for both of these earthquakes (i.e., toward the east and GV06) confirms more easterly epicentral locations compared to the 26 June 2018 event (e.g., [*Sandanbata et al.*, 2021]).

Bell et al. [2021c] estimated co-seismic displacements from the 30-sec kinematic solutions for the three largest earthquakes, which indicate there was a net uplift of ~2.0 m at GV09 and 0.6 m at GV06 (Table 1) consistent with the kinematics of the TDF, whereby slip decreases toward the hinge in the northeast caldera. Therefore, the co-seismic displacements for the entire eruptive cycle (i.e., for the pre- and co-eruptive phases) clearly show that net slip on the southern TDF was upward (i.e., uplift of the Sinuous Ridge and resurgence of the caldera), not the -1.1 to -0.3 m subsidence as suggested by *Shreve and Delgado* [2023] based on modeling of model residuals for *only* the co-eruptive period. Furthermore, our results indicate that resurgence has been the dominant volcano-tectonic process at Sierra Negra during the last two eruption cycles and has been located in the same region of the caldera; the ~2.0 m of net uplift observed at GV09 in 2018 and the ~2.5 m observed in 2005 were both located near the southwestern corner of the TDF (Figure 2; [*Chadwick et al.*, 2006]).

3 Seismic Moment Release

A simple test of the proposed hypothesis that caldera collapse was initiated during the 2018 eruption [*Shreve and Delgado*, 2023] is to compare the total seismic moment released during the pre-eruptive and co-eruptive phases. The 26 June 2018 M_w 5.3 earthquake, which uplifted the Sinuous Ridge, dominates the seismic moment release by approximately one order of magnitude (Table 1; [*Sandanbata et al.*, 2021]). *Shreve and Delgado* [2023] suggest that the ~2 m difference between the measured pre-eruption uplift of ~6.5 m and co-eruptive subsidence of ~-8.5 m was accommodated by slip on the TDF and that any residual between their modeled slip and this amount was accommodated by aseismic slip on the TDF. There are several problems with this analysis. First, in their modeling of the co-eruptive deflation, they solve for the total ~8.5 m of subsidence as elastic deformation, and thus 2 m of potential slip are not available. Second, aseismic slip was not detected in the cGPS time series. Finally, the estimated magnitude of aseismic slip presented by *Shreve and Delgado* [2023] is low (i.e., ~0.1 m) and therefore net slip on the TDF would still be positive (i.e., uplift of the Sinuous Ridge and resurgence).

4 Geologic Evidence for Caldera Resurgence

The Sierra Negra caldera formed by displacement on a vertical to inward dipping ring fault system with secondary faults dipping outward (Figure 1; see [*Acocella et al.*, 2024; *Reynolds et al.*, 1995]). The Sinuous Ridge formed by reactivation and repeated uplift on the secondary faults (i.e., the TDF system) [*Acocella et al.*, 2024; *Reynolds et al.*, 1995]. The caldera behaves elastically during pre-eruptive uplift and co-eruptive deflation phases, and these phases of deformation stress the TDF leading to seismic failure (e.g., [*Chadwick et al.*, 2006; *Gregg et al.*, 2018]). [*Bell et al.*, 2021a; *Bell et al.*, 2021c] showed: 1) earthquakes on the TDF do not change inflation or deflation rates of the magmatic reservoir; and 2) inelastic deformation and seismicity were restricted to the TDF during pre-eruptive inflation and co-eruptive deflation (see Figures 2, 3 & 5 of [*Bell et al.*, 2021c]). That is, no measurable deformation or seismicity occurred along the caldera-bounding ring fault, and no surface ruptures have been observed on the caldera ring fault during either the 2005 or 2018 eruptions. Furthermore, the last two eruptive cycles resulted in net uplift of the Sinuous Ridge caused by co-seismic displacements on the TDF system, including ~2.5 m preceding the 2005 eruption [*Chadwick et al.*, 2006] and ~2.0 m net displacement during the 2018 eruption (Table 1 and earlier discussion). Field observations of part of these co-seismic displacements along the TDF faults can be seen in Figure 2, where segments of the surface ruptures from the 10 October 2005 M_w5.5 and 26 June 2018 M_w5.3 events are shown.

Finally, *Shreve and Delgado* [2023] compare the 2018 eruption to the 2014 Bardarbunga, Iceland and 2018 Ambrym, Vanuatu events. In the Bardarbunga case, they make the assumption that all calderas with trapdoor faulting are created equal. The Trapdoor Fault system at Sierra Negra is not the same as “trapdoor faulting” at Bardarbunga, Iceland. Trapdoor faulting at Bardarbunga occurs along the caldera bounding ring fault, not on an intra-caldera fault system [*Gudmundsson et al.*, 2016]; thus, it is simply asymmetric subsidence of the caldera. Additionally, one should not expect the same style of deformation at these two basaltic calderas, as they have dramatically different roof thickness to diameter ratios, which dictates caldera deformation (i.e., 0.22-0.28 at Sierra Negra and 1.0-1.5 at Bardarbunga; see *Holohan et al.* [2011] for a discussion). In the Ambrym case, the authors suggest that because it has been hypothesized that the caldera formed incrementally (see [*Hamling et al.*, 2019; *Shreve et al.*, 2021]), the caldera at Sierra Negra has also formed in this manner. When and how the caldera at Sierra Negra formed is an open question. The nearby Fernandina caldera collapsed >300 m in one, dramatic event in 1968 [*Simkin and Howard*, 1970]. Could Sierra Negra also experience caldera collapse in this style?

5 Conclusions

Over the last two decades, detailed observations of basaltic caldera-forming eruptions have led to new insights into the processes of caldera formation. However, detailed evidence of caldera resurgence of a basaltic caldera system have only been observed at Sierra Negra caldera [*Acocella et al.*, 2024; *Bell et al.*, 2021c; *Chadwick et al.*, 2006], whereby the inner caldera has grown vertically along the 14 km long, C-shaped Sinuous Ridge created by near-vertical displacements on the intra-caldera TDF. Repeated eruptive cycles with trapdoor faulting earthquakes have generated the 150 m high Sinuous Ridge that now rises 50 m above the southwestern caldera rim (Figure 1). In contrast to the process of caldera collapse, which results from the evacuation of magma from a subsurface reservoir, resurgence at Sierra Negra has happened during the pre-eruptive phase of multiple eruptive cycles. For example, the last two eruptive cycles resulted in net uplift of the Sinuous Ridge – TDF system, including ~2.5 m preceding the 2005 eruption [*Chadwick et al.*, 2006] and ~2.0 m net displacement during the 2018 eruption. Inflation of the magma reservoir at 2 km depth imparts stress on the TDF until the fault ruptures during the pre-eruptive phase of activity. The larger magnitude (>M5) pre-eruptive earthquakes (e.g., the 2005 M_w5.4 and 2018 M_w5.3) change the state of stress on the volcano-tectonic system, opening pathways for magma intrusion and eruption [*Bell et al.*, 2021c; *Gregg et al.*, 2018; *Gregg et al.*, 2022]. These observations highlight the interplay and dynamics of the magma-volcano-tectonic system at Sierra Negra.

In an attempt to put their observations into the context of other recent caldera forming events, *Shreve and Delgado* [2023] did not account for important observations presented in [*Bell et al.*, 2021a; *Bell et al.*, 2021b; *Bell et al.*, 2021c]. By focusing on the co-eruptive deformation and not including the pre-eruptive seismicity and deformation, the conclusions of *Shreve and Delgado* [2023] regarding caldera collapse are incorrect. In the context of recent, well-monitored basaltic caldera-forming eruptions (e.g., 2000 Miyakejima, Japan [*Geshi et al.*, 2002], 2014 Bardarbunga, Iceland [*Gudmundsson et al.*, 2016], and 2018 Kilauea, USA [*Neal et al.*, 2019]), measurement of net caldera uplift (i.e., resurgence) at Sierra Negra is in striking contrast. The rarity of resurgence at basaltic calderas makes the 2005 to 2018 eruption cycle an especially important event to study and understand.

Acknowledgements

The authors thank the Editor, Associate Editor and two reviewers for their thoughtful comments. PCL (EAR-2122744), PMG (EAR 2122745), and AFB (NE/W007274/1) were supported by an NSFGEO-NERC award to study Sierra Negra volcano.

References

Acocella, V., F. Galetto, F. Amelung, and S. Aguaiza (2024), Sierra Negra, Galápagos: A resurgent-block basaltic caldera, *GSA Bulletin*, *137*(3-4), 1703-1716, doi:10.1130/b37799.1.

Amelung, F., S. Jonsson, H. Zebker, and P. Segall (2000), Widespread uplift and 'trapdoor' faulting on Galapagos volcanoes observed with radar interferometry, *Nature*, *407*(6807), 993-996, doi:10.1038/35039604.

Bell, A. F., S. Hernandez, P. C. La Femina, and M. C. Ruiz (2021a), Uplift and Seismicity Driven by Magmatic Inflation at Sierra Negra Volcano, Galapagos Islands, *Journal of Geophysical Research-Solid Earth*, *126*(7), doi:10.1029/2021jb022244.

Bell, A. F., S. Hernandez, J. McCloskey, M. Ruiz, P. C. LaFemina, C. J. Bean, and M. Mollhoff (2021b), Dynamic earthquake triggering response tracks evolving unrest at Sierra Negra volcano, Galapagos Islands, *Science Advances*, *7*(39), doi:10.1126/sciadv.abh0894.

Bell, A. F., et al. (2021c), Caldera resurgence during the 2018 eruption of Sierra Negra volcano, Galapagos Islands, *Nature Communications*, *12*(1), doi:10.1038/s41467-021-21596-4.

Branney, M. J. (1995), DOWNSAG AND EXTENSION AT CALDERAS - NEW PERSPECTIVES ON COLLAPSE GEOMETRIES FROM ICE-MELT, MINING, AND VOLCANIC SUBSIDENCE, *Bulletin of Volcanology*, *57*(5), 303-318, doi:10.1007/bf00301290.

Branney, M. J., and V. Acocella (2015), Chapter 16 - Calderas, in *The Encyclopedia of Volcanoes (Second Edition)*, edited by H. Sigurdsson, pp. 299-315, Academic Press, doi:https://doi.org/10.1016/B978-0-12-385938-9.00016-X.

Brothelande, E., et al. (2016), Structure and evolution of an active resurgent dome evidenced by geophysical investigations: The Yenkahe dome-Yasur volcano system (Siwi caldera, Vanuatu), *Journal of Volcanology and Geothermal Research*, *322*, 241-262, doi:https://doi.org/10.1016/j.jvolgeores.2015.08.021.

Chadwick, W. W., D. J. Geist, S. Jonsson, M. Poland, D. J. Johnson, and C. M. Meertens (2006), A volcano bursting at the seams: Inflation, faulting, and eruption at Sierra Negra volcano, Galapagos, *Geology*, *34*(12), 1025-1028, doi:10.1130/g22826a.1.

de Silva, S. L., A. E. Mucek, P. M. Gregg, and I. Pratomo (2015), Resurgent Toba—field, chronologic, and model constraints on time scales and mechanisms of resurgence at large calderas, *Frontiers in Earth Science*, *3*, doi:10.3389/feart.2015.00025.

Dziewonski, A. M., T.-A. Chou, and J. H. Woodhouse (1981), Determination of earthquake source parameters from waveform data for studies of global and regional seismicity, *Journal of Geophysical Research: Solid Earth*, *86*(B4), 2825-2852, doi:https://doi.org/10.1029/JB086iB04p02825.

Ekström, G., M. Nettles, and A. M. Dziewoński (2012), The global CMT project 2004–2010: Centroid-moment tensors for 13,017 earthquakes, *Physics of the Earth and Planetary Interiors*, *200-201*, 1-9, doi:https://doi.org/10.1016/j.pepi.2012.04.002.

Galetto, F., V. Acocella, and L. Caricchi (2017), Caldera resurgence driven by magma viscosity contrasts, *Nature Communications*, *8*, doi:10.1038/s41467-017-01632-y.

Galetto, F., M. Bagnardi, V. Acocella, and A. Hooper (2019), Noneruptive Unrest at the Caldera of Alcedo Volcano (Galapagos Islands) Revealed by InSAR Data and Geodetic Modeling, *Journal of Geophysical Research-Solid Earth*, *124*(4), 3365-3381, doi:10.1029/2018jb017103.

Geist, D., W. Chadwick, and D. Johnson (2006), Results from new GPS and gravity monitoring networks at Fernandina and Sierra Negra Volcanoes, Galapagos, 2000-2002, *Journal of Volcanology and Geothermal Research*, *150*(1-3), 79-97, doi:10.1016/j.jvolgeores.2005.07.003.

Geist, D., K. S. Harpp, T. R. Naumann, M. Poland, W. W. Chadwick, M. Hall, and E. Rader (2008), The 2005 eruption of Sierra Negra volcano, Galapagos, Ecuador, *Bulletin of Volcanology*, *70*(6), 655-673, doi:10.1007/s00445-007-0160-3.

Geshi, N., T. Shimano, T. Chiba, and S. Nakada (2002), Caldera collapse during the 2000 eruption of Miyakejima Volcano, Japan, *Bulletin of Volcanology*, *64*(1), 55-68, doi:10.1007/s00445-001-0184-z.

Gregg, P. M., H. Le Mevel, Y. Zhan, J. Dufek, D. Geist, and W. W. Chadwick (2018), Stress Triggering of the 2005 Eruption of Sierra Negra Volcano, Galapagos, *Geophysical Research Letters*, *45*(24), 13288-13297, doi:10.1029/2018gl080393.

Gregg, P. M., Z. Yan, F. Amelung, D. Geist, P. Mothes, S. Koric, and Y. J. Zhang (2022), Forecasting mechanical failure and the 26 June 2018 eruption of Sierra Negra Volcano, Galapagos, Ecuador, *Science Advances*, *8*(22), doi:10.1126/sciadv.abm4261.

Gudmundsson, M. T., et al. (2016), Gradual caldera collapse at Bardarbunga volcano, Iceland, regulated by lateral magma outflow, *Science*, *353*(6296), doi:10.1126/science.aaf8988.

Hamling, I. J., S. Cevuard, and E. Garaebiti (2019), Large-Scale Drainage of a Complex Magmatic System: Observations From the 2018 Eruption of Ambrym Volcano, Vanuatu, *Geophysical Research Letters*, *46*(9), 4609-4617, doi:https://doi.org/10.1029/2019GL082606.

Holohan, E. P., M. P. J. Schöpfer, and J. J. Walsh (2011), Mechanical and geometric controls on the structural evolution of pit crater and caldera subsidence, *Journal of Geophysical Research-Solid Earth*, *116*, doi:10.1029/2010jb008032.

Jonsson, S. (2009), Stress interaction between magma accumulation and trapdoor faulting on Sierra Negra volcano, Galapagos, *Tectonophysics*, *471*(1-2), 36-44, doi:10.1016/j.tecto.2008.08.005.

Jonsson, S., H. Zebker, and F. Amelung (2005), On trapdoor faulting at Sierra Negra volcano, Galapagos, *Journal of Volcanology and Geothermal Research*, *144*(1-4), 59-71, doi:10.1016/j.jvolgeores.2004.11.029.

Marsh, B. D. (1984), On the mechanics of caldera resurgence, *Journal of Geophysical Research: Solid Earth*, *89*(B10), 8245-8251, doi:https://doi.org/10.1029/JB089iB10p08245.

Métrich, N., et al. (2011), Magma and Volatile Supply to Post-collapse Volcanism and Block Resurgence in Siwi Caldera (Tanna Island, Vanuatu Arc), *Journal of Petrology*, *52*(6), 1077-1105, doi:10.1093/petrology/egr019.

Neal, C. A., S. Brantley, L. Antolik, J. Babb, M. Burgess, K. Calles, M. Cappos, J. Chang, S. Conway, and L. Desmither (2019), The 2018 rift eruption and summit collapse of Kīlauea Volcano, *Science*, *363*(6425), 367-374.

Reynolds, R. W., D. Geist, and M. D. Kurz (1995), PHYSICAL VOLCANOLOGY AND STRUCTURAL DEVELOPMENT OF SIERRA-NEGRA VOLCANO, ISABELA-ISLAND, GALAPAGOS ARCHIPELAGO, *Geological Society of America Bulletin*, *107*(12), 1398-1410, doi:10.1130/0016-7606(1995)107<1398:Pvasdo>2.3.Co;2.

Sandanbata, O., H. Kanamori, L. Rivera, Z. W. Zhan, S. Watada, and K. Satake (2021), Moment Tensors of Ring-Faulting at Active Volcanoes: Insights Into Vertical-CLVD Earthquakes at the Sierra Negra Caldera, Galapagos Islands, *Journal of Geophysical Research-Solid Earth*, *126*(6), doi:10.1029/2021jb021693.

Shreve, T., and F. Delgado (2023), Trapdoor Fault Activation: A Step Toward Caldera Collapse at Sierra Negra, Galapagos, Ecuador, *Journal of Geophysical Research-Solid Earth*, *128*(5), doi:10.1029/2023jb026437.

Shreve, T., R. Grandin, D. Smittarello, V. Cayol, V. Pinel, M. Boichu, and Y. Morishita (2021), What Triggers Caldera Ring-Fault Subsidence at Ambrym Volcano? Insights From the 2015 Dike Intrusion and Eruption, *Journal of Geophysical Research: Solid Earth*, *126*(6), e2020JB020277, doi:https://doi.org/10.1029/2020JB020277.

Simkin, T., and K. A. Howard (1970), Caldera Collapse in the Galápagos Islands, 1968: The largest known collapse since 1912 followed a flank eruption and explosive volcanism within the caldera, *Science*, *169*(3944), 429-437.

Vasconez, F. J., P. Ramón, S. Hernandez, S. Hidalgo, B. Bernard, M. Ruiz, A. Alvarado, P. La Femina, and G. Ruiz (2018), The different characteristics of the recent eruptions of Fernandina and Sierra Negra volcanoes (Galápagos, Ecuador), *Volcanica*, *1*(2), 127-133.

Yun, S., P. Segall, and H. Zebker (2006), Constraints on magma chamber geometry at Sierra Negra Volcano, Galapagos Islands, based on InSAR observations, *Journal of Volcanology and Geothermal Research*, *150*(1-3), 232-243, doi:10.1016/j.jvolgeores.2005.07.009.

Figures

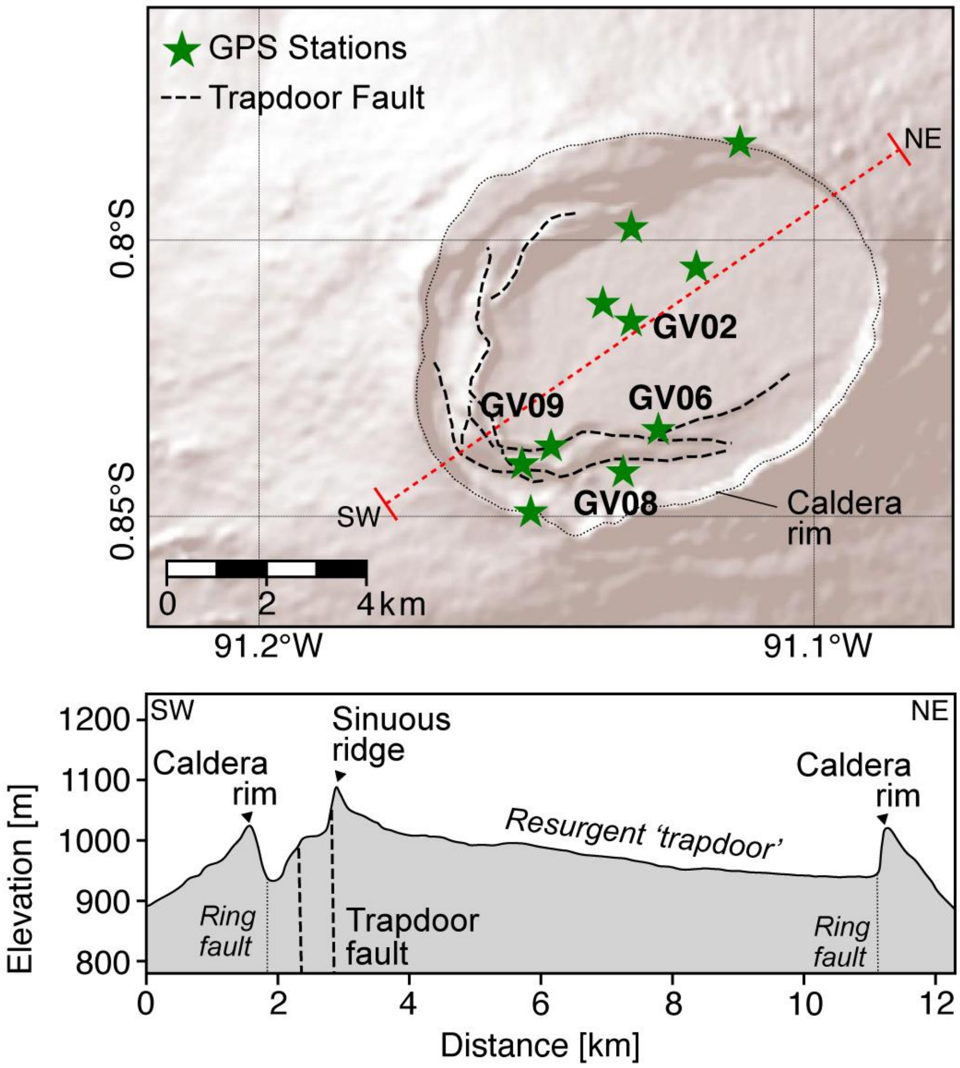

Figure 1. Top) Topographic map of Sierra Negra volcano indicating the Trapdoor Fault system (black dashed lines), and the location of cGPS stations operating during the 2018 eruption (green stars). Red dashed line indicates the location of the topographic cross-section shown in the bottom panel. Bottom) Topographic profile across the caldera showing the ring fault and the Sinuous Ridge, formed by displacement on the steeply-dipping Trapdoor Fault. Note the Sinuous Ridge rises ~50 m above the caldera rim. Figure modified from *Bell et al.* [2021c].

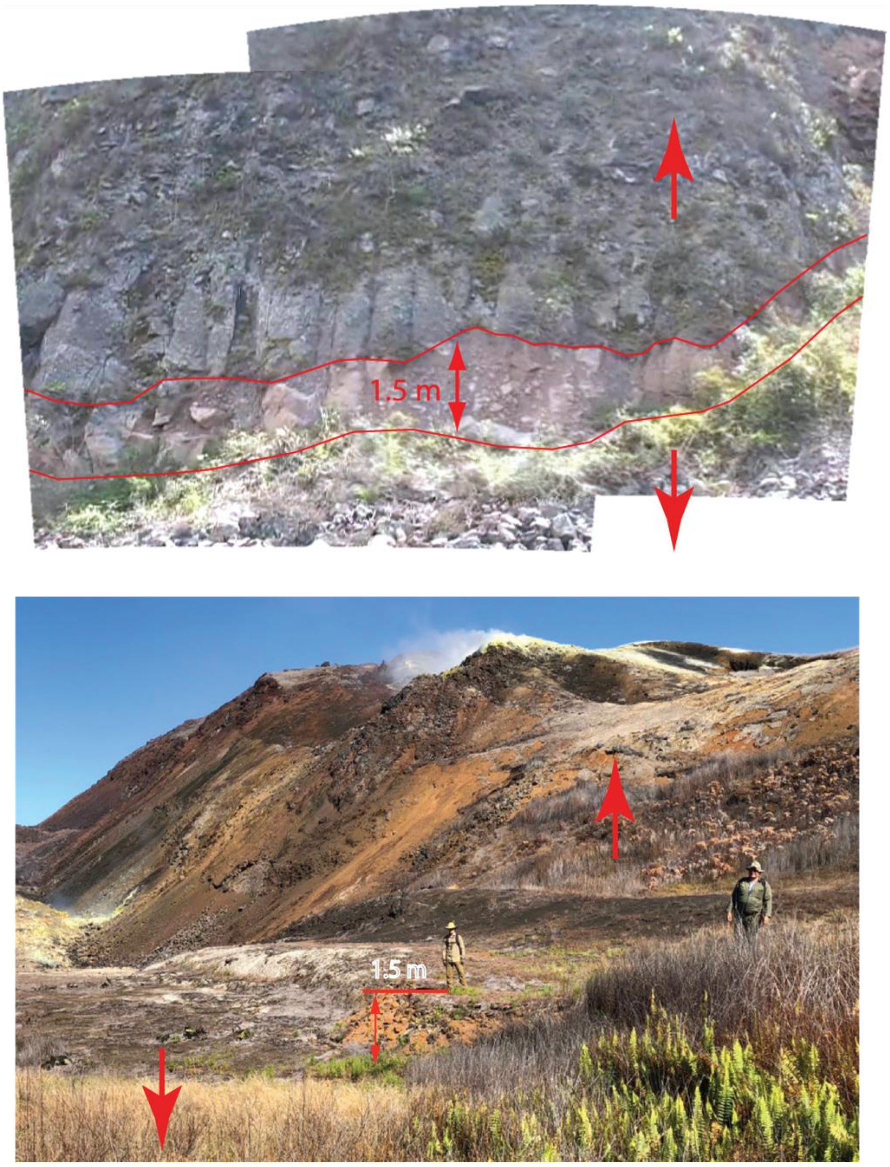

Figure 2. Photos of surface ruptures caused by co-seismic fault displacements for the 2005 (top) and 2018 (bottom) pre-eruptive earthquakes. In both cases, the pre-eruptive earthquakes caused ~1.5 m of surface displacements along the TDF. Note cGPS observations indicate >2.0 m net uplift for the 2018 event (See Figure 4). Photos from D. Geist and B. Chadwick (top) and J. Galetzka (bottom).

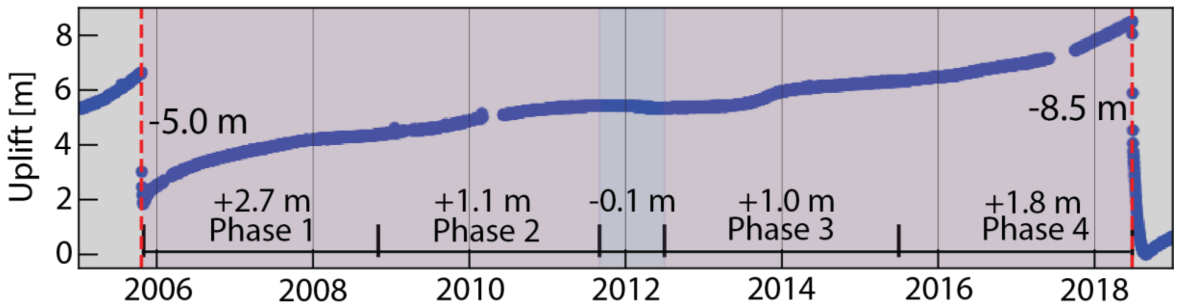

Figure 3. Composite vertical component time series for stations GV02 and GV04 located near the center of Sierra Negra caldera. The stations are located ~400 m apart and capture the complete deformation cycle between the 2005 and 2018 eruptions. The time series are relative to GV01 and combined because GV02 malfunctioned in early 2012. Note the four phases of uplift and the period (~0.5 yrs) of minor deflation in 2012. Red dashed lines mark the 22 October 2005 and 26 June 2018 eruptions. The co-eruptive deflation signals are also shown.

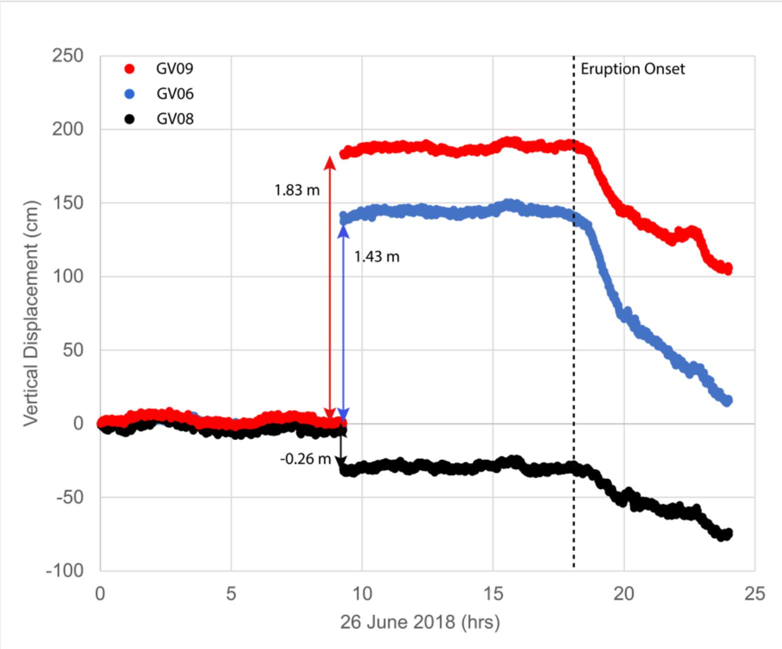

Figure 4. High-rate (30 sec) time series of the vertical component for cGPS stations GV09, GV08, and GV06 on June 26, 2018. The position time series captured the co-seismic displacement across the TDF due to the M_w 5.3 earthquake at 9:15. Estimates of the co-seismic displacement at each station are provided. The onset of the eruption is observed by the onset of rapid deflation at all stations (vertical black dashed line). See Figure 1 for station locations.

Table 1. M_w >4.5 pre- and co-eruptive earthquakes at Sierra Negra volcano in 2018.

Date	Time	M_w	M_0 (dyne-cm)‡	Displacements (m)†			Total Throw (m)	
				GV09	GV06	GV08	GV09	GV06
26-06-2018	9:15:37‡	5.3‡	1.28e+24	1.83	1.43	-0.26	2.09	1.69
05-07-2018	0:30:28‡	5.1‡	4.76e+23	-0.14	-0.71	0.14	0.0	-0.57
22-07-2018	19:49:18*	4.6 M_b*		-0.08	-0.13	0.03	-0.05	-0.10
Net Offset (m)				1.61	0.59	-0.09	2.04	1.02

* United States Geological Survey – National Earthquake Information Center
‡ Global Centroid Moment Tensor catalog
† Displacements were estimated using 30-sec kinematic solutions of the cGPS data.
Total throw is the difference between GV09 and GV08, and GV06 and GV08, as these station pairs cross the TDF fault scarps.

Figure 1.

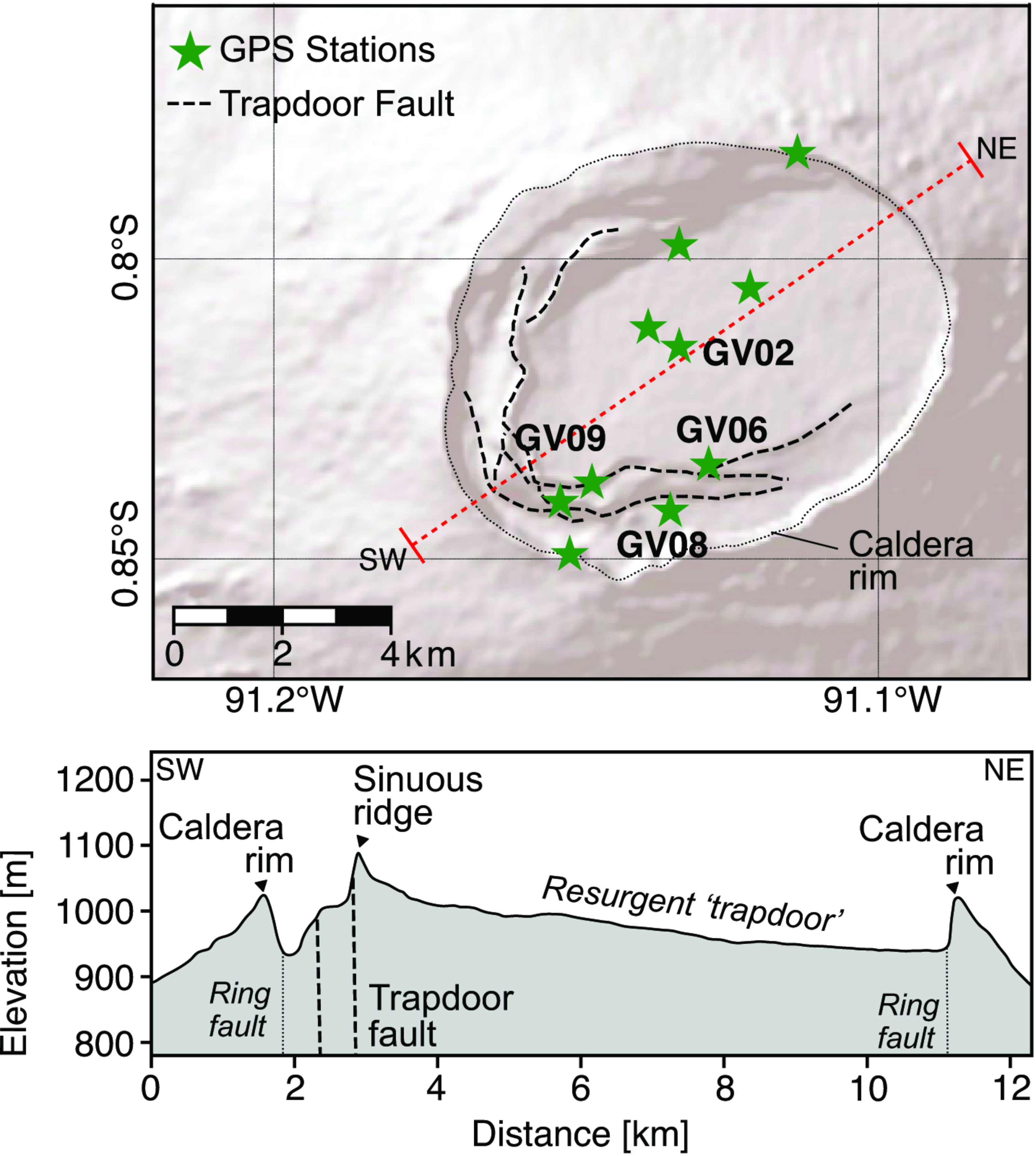

GPS Stations
Trapdoor Fault
NE
SW
GV02
GV09
GV06
GV08
Caldera rim
0.8°S
0.85°S
0
2
4 km
91.2°W
91.1°W
SW
NE
Sinuous ridge
Caldera rim
Caldera rim
Resurgent 'trapdoor'
Ring fault
Trapdoor fault
Ring fault
Elevation [m]
1200
1100
1000
900
800
0
2
4
6
8
10
12
Distance [km]

Figure 2.

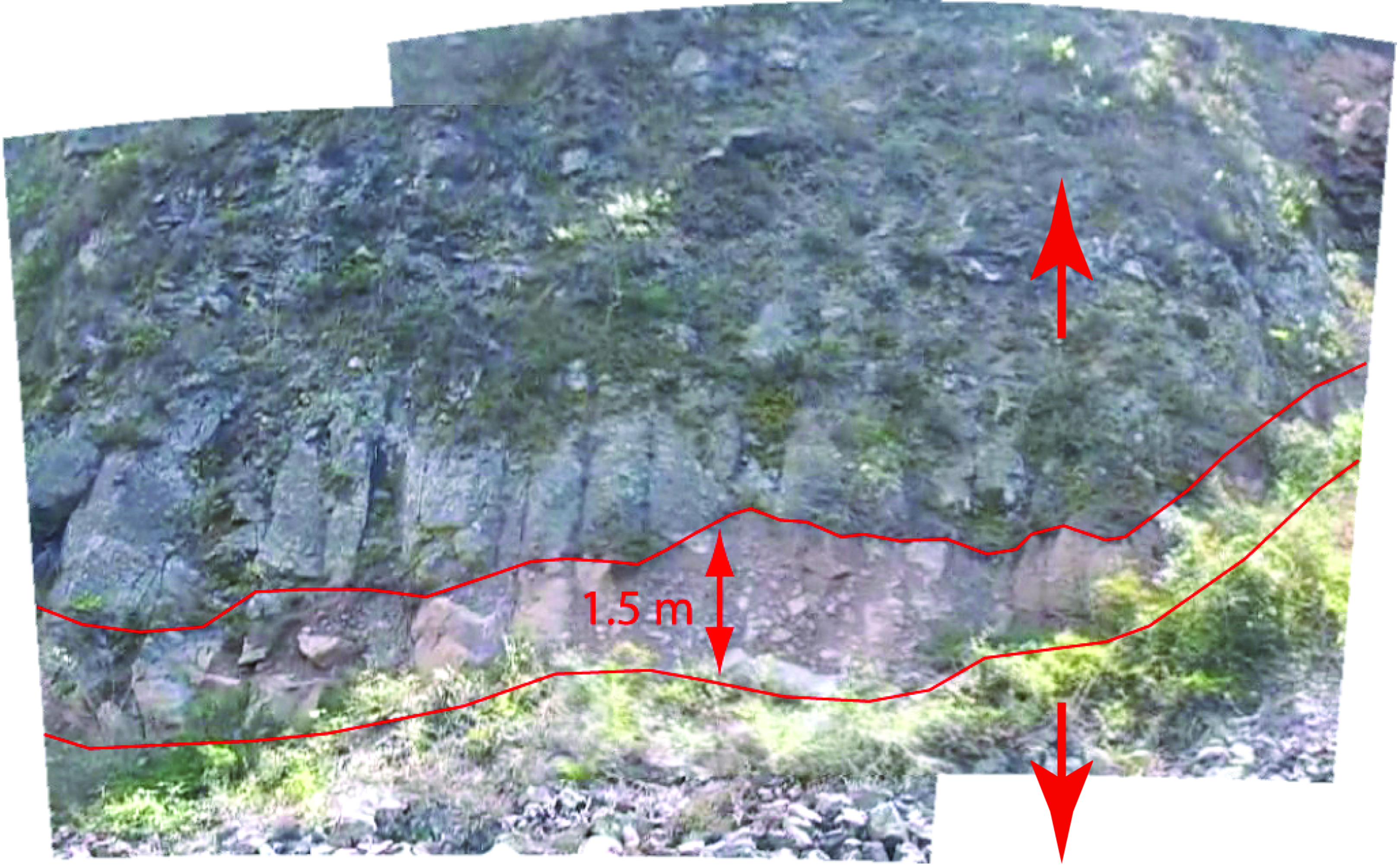
1.5 m

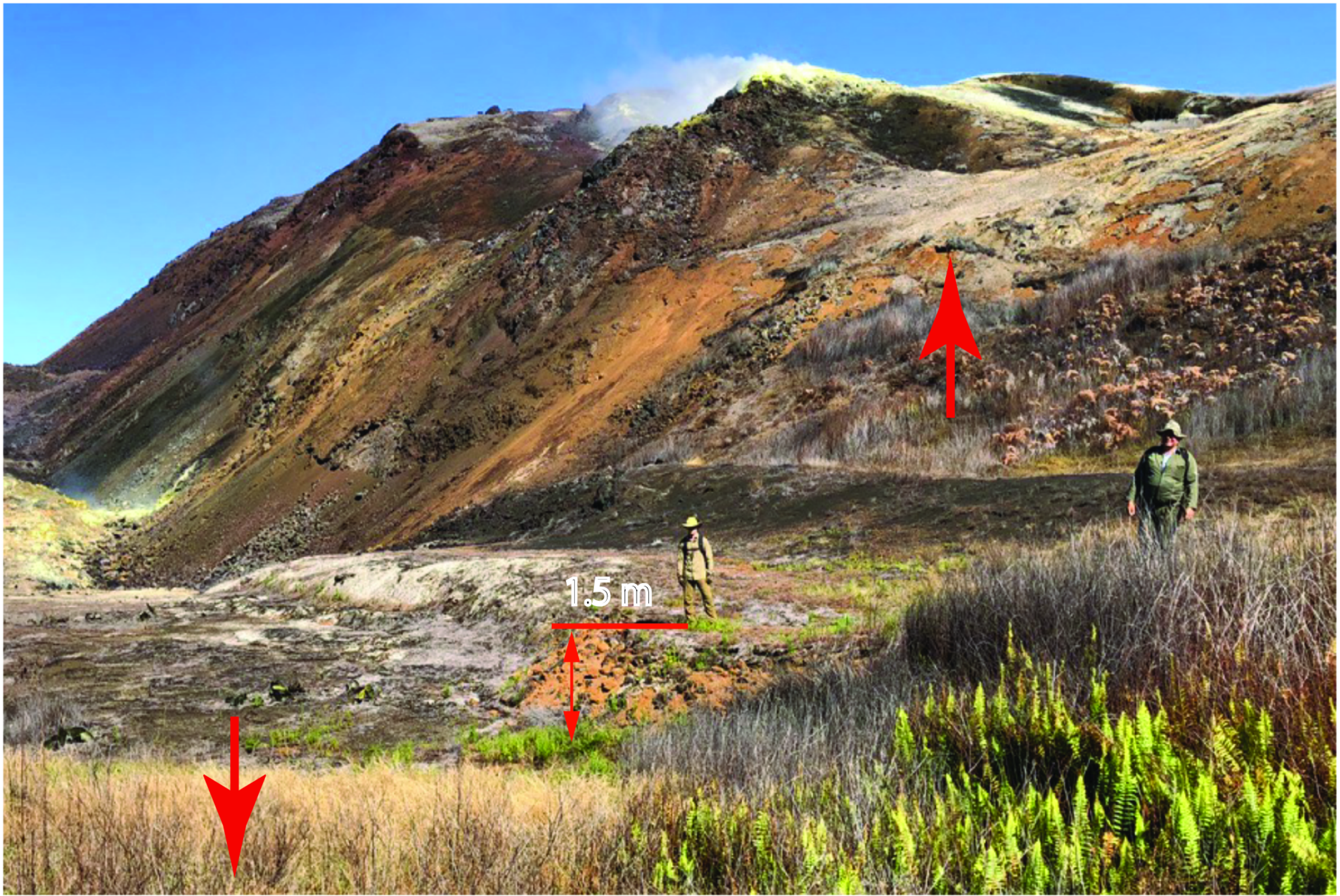
1.5 m

Figure 3.

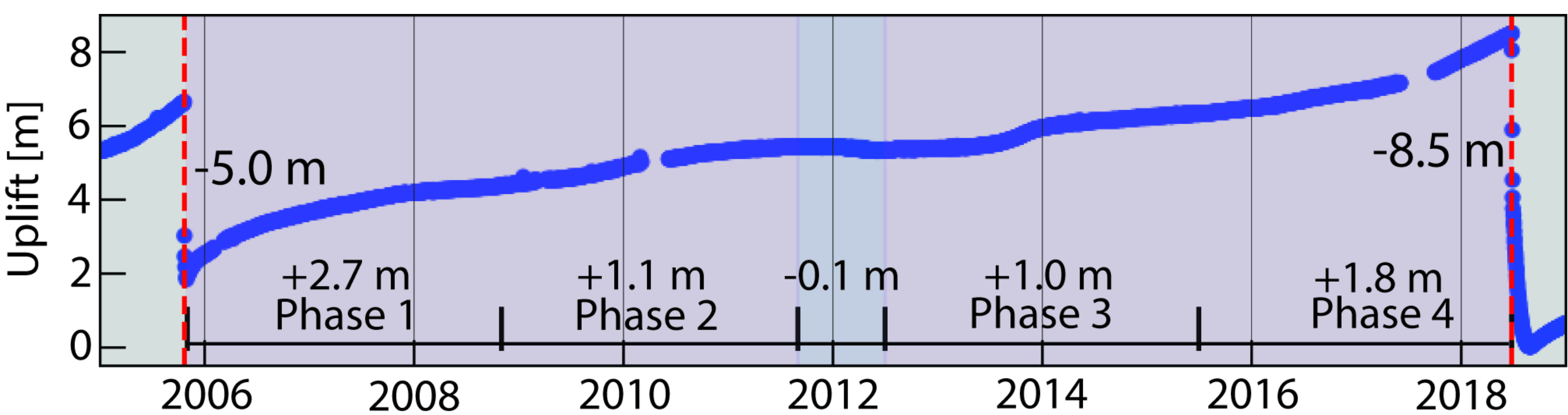

Uplift [m]
8
6
4
2
0
-5.0 m
-8.5 m
+2.7 m
Phase 1
+1.1 m
Phase 2
-0.1 m
+1.0 m
Phase 3
+1.8 m
Phase 4
2006
2008
2010
2012
2014
2016
2018

Figure 4.

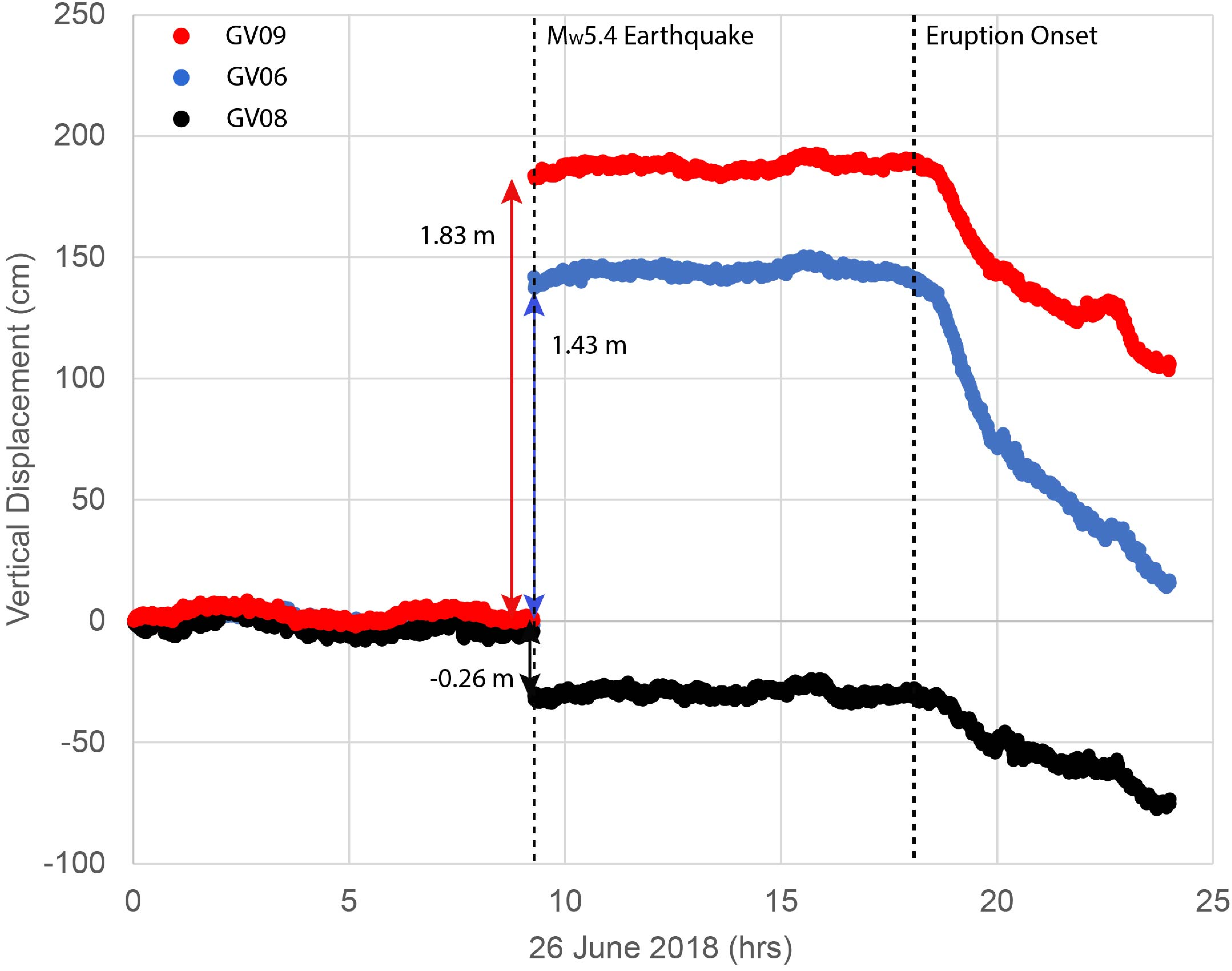

GV09
GV06
GV08
Mw5.4 Earthquake
Eruption Onset
1.83 m
1.43 m
-0.26 m
Vertical Displacement (cm)
26 June 2018 (hrs)
250
200
150
100
50
0
-50
-100
0
5
10
15
20
25